THE EFFECTS OF IRON SUPPLEMENTATION ON PRIMARY PRODUCERS IN THE WESTERN EQUATORIAL PACIFIC OCEAN

University of Washington - School of Oceanography

Michael Yurecko
myurecko@uw.edu

Abstract

This study investigates the effect of iron (FeCl3) incubation on phytoplankton growth in the western Equatorial Pacific, an area known for its high-nutrient, low-chlorophyll (HNLC) conditions, which limit primary production. The El Niño-Southern Oscillation (ENSO) shifts between El Niño and La Niña, with neutral periods between them. During El Niño, nutrient availability is decreased, leading to a lack of primary production. Iron is an essential nutrient for primary production, and the western Equatorial Pacific is known for its low iron availability. Therefore, I hypothesize that FeCl3 incubation will increase phytoplankton growth. To test this hypothesis, I collected water from various stations in the western Equatorial Pacific and incubated it with FeCl3. I monitored phytoplankton growth and nutrient concentrations through chlorophyll measurements and size fractionation. My results showed that FeCl3 incubation increased phytoplankton growth, supporting my hypothesis. Furthermore, I used a dilute acid test to determine chlorophyll-a concentration in the stimulated chlorophyll colonies. My results suggest that iron is a limiting ingredient in the western equatorial Pacific, and bioavailable iron increased phytoplankton biomass. In conclusion, my study provides evidence that iron incubation can enhance phytoplankton growth in HNLC regions of the western Equatorial Pacific. My findings suggest that iron availability is critical in regulating primary production in these areas. Understanding the biogeochemical processes that control primary production in HNLC regions can provide essential insights into global climate change and biogeochemical cycling.

Plain Language Summary

This study explored whether adding iron (FeCl3) to water in the western Equatorial Pacific can increase the growth of tiny, pigmented organisms called phytoplankton. This area is known for being low in nutrients that limit biological growth. During El Niño, nutrient availability decreases even more, leading to less biological growth. Iron is an essential nutrient for these organisms, but it is usually scarce in this part of the ocean. I hypothesized that adding FeCl3 would increase phytoplankton growth. As the researcher, I collected water from different stations and incubated it with FeCl3. I then measured the growth of the phytoplankton and the nutrient concentrations in the water each day. The results showed that the FeCl3 did increase phytoplankton growth, supporting the hypothesis. The study also suggests that iron is a limiting factor for phytoplankton growth in this area. Understanding how to increase plant growth in these low-nutrient regions can help us better understand global climate change and biogeochemical cycling.

Introduction

The El Nino/Southern Oscillation (ENSO) is a phenomenon that describes the interaction between weather perturbations in the equatorial Pacific and the recurrent oceanic response. Generally, the ENSO shifts between El Nino and La Nina every three to seven years, with times of neutrality in transition periods. Although these transitions are rarely observed *in situ,* but valuable for visualization. A “neutral” tropical Pacific weather pattern would consist of *average* sea surface temperatures, *average* precipitation, and *average* trade wind strength. These would be times when neither La Nina nor El Nino conditions are the dominant weather patterns

meaning their characteristics are near their long-term averages. Therefore, neutrality in the ENSO is more qualitative than quantitative, as they are an estimated average between below-normal (La Nina) and above-normal (El Nino) measurements, which update upon occurrence. ENSO events largely dictate ocean fluid circulation, directly affecting the atmosphere and global precipitation behavior.

Previously, *in situ,* physical measurements combined with MODIS (Moderate Resolution Imaging Spectroradiometer), a NASA-operated chlorophyll-sensitive satellite, had reliably predicted areas along the equatorial Pacific that are either low in chlorophyll or observed low net primary production (NPP). This is unusual behavior in primary producers when primary producers have a surplus of nutrients due to upwelling and dramatically reduced residence time. In such cases, these ocean regions are considered high-nutrient low-chlorophyll (HNLC) and are the primary motivation for this research.

Phytoplankton are hypothesized to be responsible for the massive global increase in oxygen in the Paleoproterozoic era, coined the “Great Oxygenation Event” (Gumsley et al., 2017). Like most organisms that can photosynthesize, phytoplankton takes carbon dioxide from the atmosphere and converts it into sugar and breathable oxygen. One in every two breaths inhaled by animals can be attributed to the photosynthetic byproducts of phytoplankton (Sudeshna et al., 2022). Therefore, fully understanding why phytoplankton does not grow in the presence of excess nutrients could dramatically change our approach to climate research while providing a further understanding of critical biogeochemical processes in a unique region of the ocean not often investigated.

Iron is an essential nutrient for primary production in the ocean and is among the fourth most common element on Earth. However, despite its relative abundance in the Earth’s

lithosphere, over one-third of all phytoplankton are limited by iron's limited oceanic concentration (Schoffman et al., 2016). Iron commonly comes in two readily available compounds: iron (II), known as ferric oxide, and iron (III), known as ferrous oxide. While each chemical compound naturally occurs in the ocean, iron (II), the most biogenically usable form, is generally scavenged long before the iron can travel into the upper mixed layer (Emerson D, 2016). This is problematic for organisms such as phytoplankton that require the reduction of iron during photosynthesis.

According to a study conducted in 2003, phytoplankton are responsible for over half of global carbon fixation (Morel et al., 2003). Despite these microorganisms' size, they do not reproduce as slowly as their photosynthetic terrestrial counterparts. In ideal conditions, some phytoplankton can double in biomass daily (Morel et al., 2003). In order for phytoplankton to use iron for photosynthesis, ultraviolet radiation must interact with seawater, thus allowing direct ligand-to-metal transfer or photochemically produced radicals (**Figure 1**), changing the oxidation state of Fe(III) to a more accessible source of Fe(II) (Lueder et al., 2020). However, Fe(III) and many other trace metals are slow to interact with phytoplankton through photochemical processes such as redox cycling, enzymatic reactions, or metal chelating ligands which may be limiting phytoplankton's biogeochemical processes in iron-limited zones.

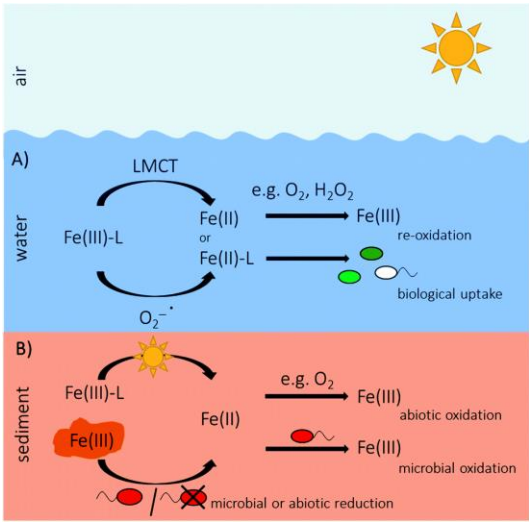

Figure 1. Biogeochemical cycle involving the sun-induced photochemical reduction of Fe(III) to Fe(II) using either ligand-to-metal charge transfer or photochemically produced radicals in an aqueous or sedimentary environment (Lueder et al., 2020).

Bioavailable nutrients, such as iron, interact physiologically with marine life and are cycled through the ocean via several trophic interactions. Depending on the point in the biogeochemical cycle, microorganisms absorb, incorporate, or excrete nutrients, while oceanic circulation pumps water throughout the water column. Algal blooms, such as those made from dinoflagellates and diatoms, will be consumed by zooplankton, then again by larger organisms, contributing to the downward flux of carbon and other nutrients. Once all labile nutrients are depleted, heterotrophic bacteria and viruses recontribute dissolved and particulate organic matter to the microbial loop and shuttle nutrients back toward the surface. Typically, the consumption of nutrients in the upper mixed layer outpaces the upward transport of remineralized elements carried by upwelling, leading to nutrient-limited zones, such as those found in some areas in the Pacific Ocean.

The Western Equatorial Pacific is one of those areas where iron is quickly depleted in the upper mixed layer. Strong winds and thermodynamically driven circulation occasionally allow warm water to pile up near South America, slowing the upwelling of cool, nutrient-dense water near Fiji. This phenomenon is powerful during El Nino, when the trade winds are no longer the dominant force of circulation on the equator. Other processes, such as Ekman transport, carry away remaining equatorial nutrients which are rapidly consumed by phytoplankton. Nevertheless, Fe(III) and Fe(II) are naturally supplemented to the ocean in several other ways. Hydrothermal ventilation in the earth's crust, runoff from riverine inputs, and Eolian deposition (wind-blown dust) are all known natural sources. However, a small amount of dissolved iron

(dFe) may be attributed to anthropogenic means via ocean transportation (**Figure 2**) (Anh et al., 2021). Biogenic iron will be considered dissolved iron (dFe) for the remainder of this paper.

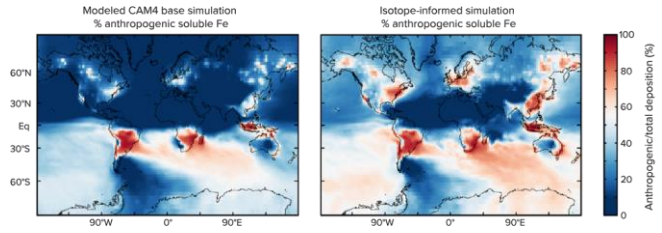

Figure 2. Simulated anthropogenic soluble Fe estimates modeled before 2019 (left) and from GEOTRACES (right) show a more accurate of Fe blown in from land. GEOTRACES is an international research program that aims to improve the understanding of biogeochemical cycles in the ocean (Underwood, 2020).

According to National Oceanographic and Atmospheric Administration (NOAA), as we transacted through the southern Pacific, we experienced a transition in the ENSO from La Nina to El Nino (EL NIÑO/SOUTHERN OSCILLATION (ENSO) DIAGNOSTIC DISCUSSION 2023). Using NASA's satellite imaging (MODIS), I observed a historical lack of primary production in the southern Pacific during El Nino. I postulate this is due to a limitation in nutrients such as iron. Thus, I hypothesize that El Nino will decrease iron availability in the western Equatorial Pacific and increase phytoplankton concentration. In contrast, nutrients will decrease because the nutrients are being incorporated into phytoplankton biomass. To test these hypotheses, I plan to supplement water samples from the western Equatorial Pacific with dFe, thus increasing the concentration of the primary producers (**Figure 3**).

To determine an accurate concentration of Chlorophyll-*a* in the water samples, I will use a variation on Carl Lorenzen's chlorophyll-*a* absorption process. I also plan to utilize dilute acid on several samples post-incubation to determine the disposition of the stimulated chlorophyll colony because active and degraded chlorophyll has an indistinguishable absorption value

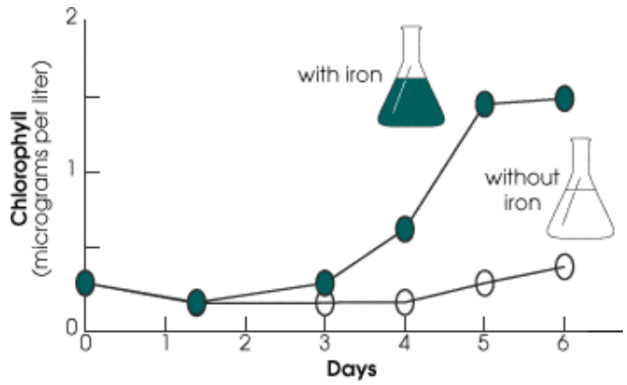

Figure 3. Three-day experimental results of chlorophyll production in seawater dosed with biogenic iron. Dr. John Martin conducted the research in his lab at Moss Landing Marine Laboratories in 1981. Dr. Martin hypothesized that iron is the limiting micronutrient in High-Chlorophyll Low-Nutrient (HCLN) zones. Results were published in Nature magazine in 1989. (National Aeronautics and Space Administration, 2001)

(~665m u). According to Carl Lorenzen, inactivated (degraded) chlorophyll will present different absorption spectra once introduced to oxalic or 1 N HCl. The reaction between the dilute acid and the chlorophyll causes the chlorophyll to release the bound magnesium molecule in the porphyrin ring, thus converting the chlorophyll-*a* to pheophytin and pheophorbide which together are considered "pheo-pigments." The pheo-pigments have a different absorption spectrum (~650m u) than Mg-bound chlorophyll which, once corrected for cell-to-cell differences, produces a concentration of active chlorophyll-*a* (Lorenzen, 1965).

Methods

Numerous procedures were constructed to reduce experimental errors and ensure accurate data collection to determine the effectiveness of iron (FeCl3) incubation on phytoplankton growth. On March 4th, 2023, water was collected from 5 degrees North, 180 degrees East, The equator, to 5 degrees South, 180 East. These stations are two, nine, and sixteen, respectively (**Figure 4.**).

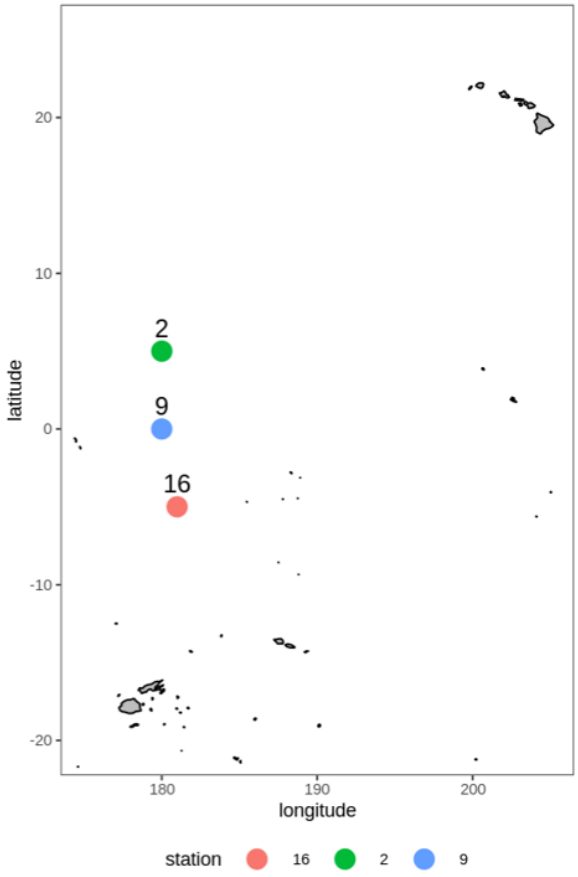

Figure 4. Map section of CTD stations 3, 9, and 16 which were transected by the Thomas V. Thompson on from March 3rd to March 7th, 2023. Stations 2, 9, and 16 are plotted showing relative latitude and longitudinal scale on their respective axis. Station "2" is 5 N, station "9" is on the equator, and station "16" is 5 S.

Water from the Deep Chlorophyll max (DCM) and water below the ship draft (approximately seven meters) was sampled using a *Stayfish* trace-metal-free pump and a 24 Niskin-bottle CTD. The DCM was determined from data relayed from the CTD to outputs displayed in real-time in the research vessel haul. Each station, such as those mentioned here, used fluorescence and beam attenuation as a proxy for primary producer concentration levels in the water column (**Figure 5.)** Once the CTD reached the predetermined DCM, a Niskin bottle was fired to capture the water and nutrient concentration drained into amber widemouthed 1L bottles. This water was labeled "Deep" and used as a biological primer for incubation.

Using a *Stayfish* trace-metal-free pump, we filled 14 two-liter clear bottles with trace-metal-free water, which were then promptly put into a cold dark storage space until they were ready for nutrient spiking. 0.5mL of 12umol FeCl3 stock solution was added to each two-liter bottle of trace-metal-free water which closely simulates the appropriate concentration of natural iron modeled to exist in the area. To ensure that FeCl3 spiked two-liter bottles would grow phytoplankton, a 19:1 dilution of "Deep" water was also spiked to the same two-liters bottles. Three "deep" spiked-only water bottles were incubated without FeCl3 and incubated to act as a control.

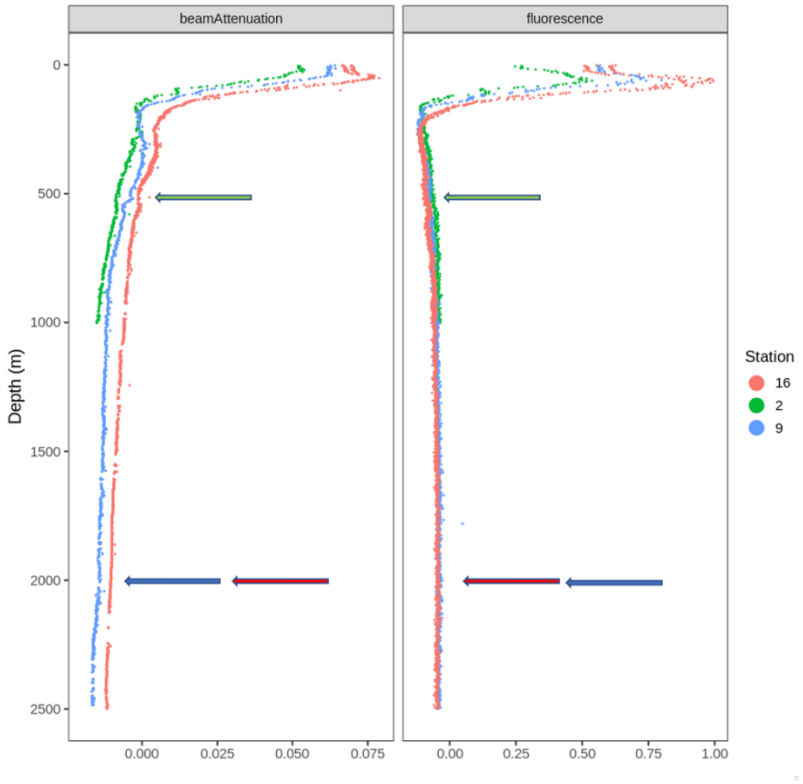

Figure 5. CTD profiles of fluorescence and beam attenuation which is used as a proxy for chlorophyll concentration within the water column. The Deep Chlorophyll Max (DCM) and the mixed layer are observed and relayed in real-time from sensors on the CTD. The marked points are where each deep-water sample, which is characterized as "5% Deep," was taken along the profile.

Once the 2L bottles were spiked with FeCl3 and 19:1 deep water, each bottle was hand agitated to reach homogeneity in nutrient levels. 100mL were drawn from each bottle before incubation for initial chlorophyll measurements and size fractionation. Once the chlorophyll samples were taken from the 2L bottles, the bottles were placed in three separate 2'x4'x1' clear plastic incubators, secured outside on the deck of the vessels (**Figure 6.**). Careful considerations ensured the incubators were in direct sunlight during sunlight hours. A nylon mesh was cut and

sewn to fit the incubators on all sides, which was measured to simulate an average light intensity of 70% surface value. After the 2L bottles were placed in the incubators, they were filled with seawater pumped from the ship's water inlet. The water was bled out the opposite side of the incubators into the sea, creating a flow of fresh seawater through the incubators. This process kept the incubated samples temperature controlled. After 24 hours, and then in 24-hour increments, the bottles were removed from the incubators and drained of 100mL of water for chlorophyll and size fractionation.

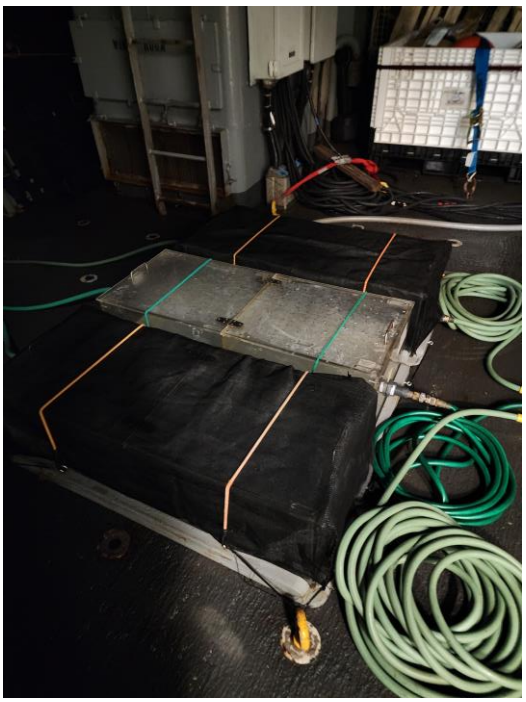

Figure 6. Three incubators sit on the Thomas V. Thompson on March 3rd, 2023. The center incubator has the mesh cover removed to better show experimental design. The hoses on the (right) side are providing water from the ships seawater inlet while the hoses on the (left) side provide a bleed off to the sea.

Chlorophyll was extracted from the 100mL sample using a 7uM filter and Millipore vacuum pump following standard chlorophyll filtration procedures (Caspers, 1970). Due to the lack of a sonicator on board, the 0.7uM filters were placed into 10mL of 90% Acetone and put into a -20deg C freezer for 24 hours. Chlorophyll readings after 24 hours elapsed were taken using a TD-700 Fluorometer, an 8-tube Centra Cl-2 centrifuge, and a Van Waters Vari-whirl shaker following the standard Lorenzen procedures measuring chlorophyll and photopigment (LORENZEN, 1967). For the 100mL that was taken for size fractionation, this water was filtered using a 4-station size fractionation tree combined with a Millipore vacuum pump and GF/F glass fiber filters (10µM, 3µM, and 0.2µM). Once the water was processed through each filter, the

filters were placed into 10mL of 90% acetone and measured for chlorophyll and phaeopigment in the same manner before.

Results

Chlorophyll concentrations post incubations were higher than initially measured at T=0, indicating a growth response from the nutrients added from the 19:1 deep water spike and FeCl3 additions. Evidence supports that the addition of FeCL3 made is statistically more significant of a change in chlorophyll concentration than the addition of 19:1 deep water alone. These results support the original hypothesis that supplementing iron with water taken from the western equatorial Pacific increases the concentration of primary producers.

Station 2

The average increase in chlorophyll concentration for the "5% Deep" treatment from T=0 to T=3, including all filter sizes, is 0.38 µg/L. In contrast, the average increase in chlorophyll concentration for the "Fe" group is 0.314 µg/L. However, compared to the control, there are significant

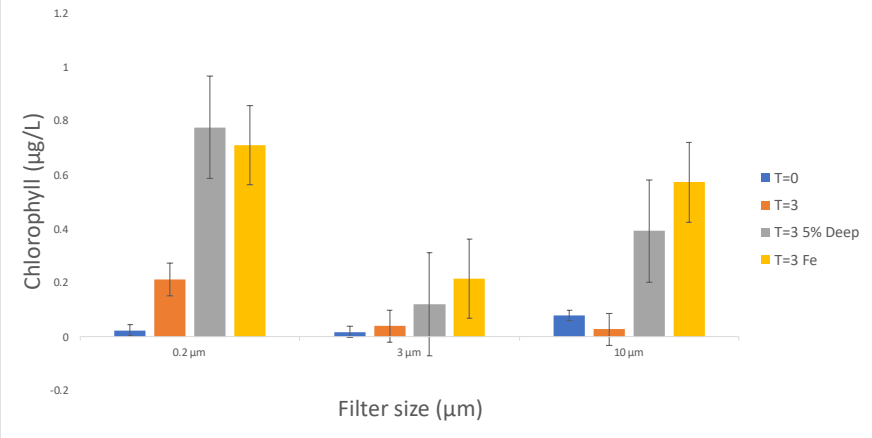

Figure 6.a. Chlorophyll incubation response data from Stations 2, 9, and 16. T1-4 were recorded in 24-hour increments. Size fractionation as represented by filter size on the axis displays data of chlorophyll processed by their representative filters. 5% deep correlates with water taken from below the mixed layer where chlorophyll concentrations are largely homogenous. Treatments from Iron and Nitrate are statistically significant from control meaning their chlorophyll response was greater than the difference of 5% deep and 5% deep and the experimental nutrient variable.

differences in the concentration of chlorophyll attributed to the treatment groups from the control. The percent increase in chlorophyll concentration for the "5% Deep" treatment group (all filter sizes) relative to the "control" group is 1236.9%, while the percent increase in chlorophyll concentration for the "Fe" treatment group (all filter sizes) relative to "control" group is 409.9%. Therefore the "5% Deep" treatment group had the highest percent increase in chlorophyll concentration relative to the "control" group from T=0 to T=3. In comparison, the "Fe" treatment group had a lower percent increase compared to the "5% Deep" treatment group but still had a substantially higher increase than the "control" group. Note that the total number of bottle and filter size combinations is 9, but for one of the combinations (bottle 3, 10 µm), the increase in chlorophyll concentration was 0 due to sampling error. Both increases in the chlorophyll concentration are significantly higher than observed in the control group. The average increase in chlorophyll concentration for the "control" treatment from T=0 to T=3, including all filter sizes, is 0.005 µg/L.

Based on the average increase in chlorophyll concentration across all three treatments and broken down by filter size, we can see that the 0.2 µm filter size had the largest increase in chlorophyll concentration for the "5% Deep" and "Fe" treatment groups at 0.78 µg/L and 0.78 µg/L respectively. In contrast, the 10 µm filter size had the largest increase in chlorophyll concentration for the "control" treatment group, which was 0.05 µg/L.

Station 9

The average increase from iron spiking on the equator (station 9) is ~ 428.3% over 96 hours. To calculate the average increase in chlorophyll with the Fe treatment from T=0 to T=4, we can subtract the chlorophyll concentration at T=0 from the concentration at T=4 and then take the average across the three filter sizes. In doing so, the average increase in chlorophyll with the

Fe treatment from T0 to T4 across all three filter sizes is 0.68 µg/L, but this increase is 428.3% higher than the increase seen in the control over 96 hours. Similarly, the control treatment saw an average increase of 72%, while the deep-water spike alone saw a 122.9% increase. The average increase in chlorophyll concentration for the Control group from T=0 to T=4 is 0.136 µg/L.

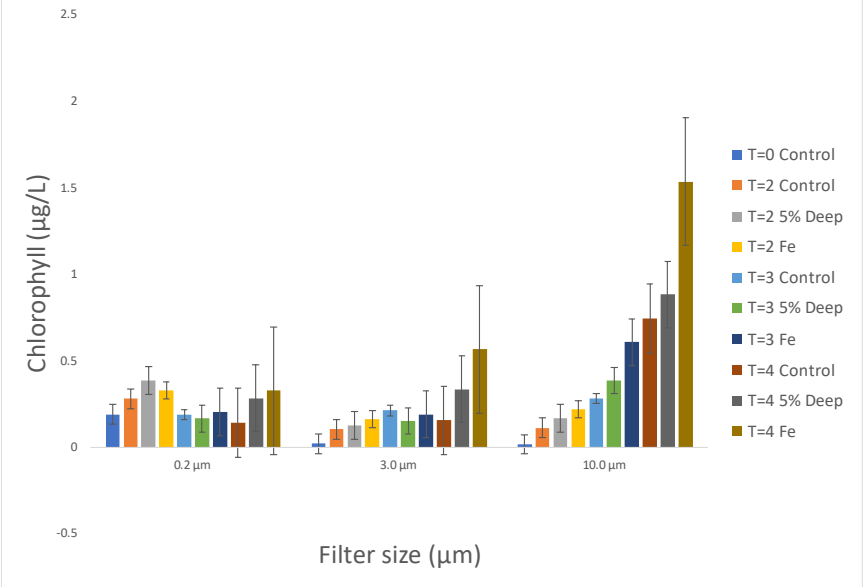

Figure 6.b. Chlorophyll incubation response data from Stations 2, 9, and 16. T1-4 were recorded in 24-hour increments. Size fractionation as represented by filter size on the axis displays data of chlorophyll processed by their representative filters. 5% deep correlates with water taken from below the mixed layer where chlorophyll concentrations are largely homogenous. Treatments from Iron and Nitrate are statistically significant from control meaning their chlorophyll response was greater than the difference of 5% deep and 5% deep and the experimental nutrient variable.

Furthermore, we can see that the 10.0 µm filter size had the largest increase in chlorophyll concentration in all three treatment groups from T=0 to T=4, with an average increase of 0.734 µg/L for the Fe treatment, 0.184 µg/L for the 5% Deep treatment, and -0.029 µg/L for the Control treatment. Note that negative values indicate a decrease in chlorophyll concentration from T=0 to T=4, while positive values indicate an increase. From this data, we can see that the 10.0 µm filter size had the largest increase in chlorophyll concentration in all three treatment groups, consistent with the previous analysis.

Station 16

The percent changes in chlorophyll concentration from T=0 to T=3 for all treatment groups use T=0 as the initial chlorophyll value. “Fe” has an average change in chlorophyll concentration from T=0 to T=3 of -0.0136 ug/L. For the 0.2 µm filter size, the control chlorophyll concentration and the 5% deep dropped 33.9% and 3.2%, while the Fe treatment increased by 42.8%. For the 3.0 µm filter size, the control, 5% deep, and Fe increased 73.1%, 135.1%, and 136.1%, respectively. For the 10 µm filter size, there was an increase from T=0 for the control, 5% deep, and Fe of 218.8%, 255.6%, and 164.3%, respectively.

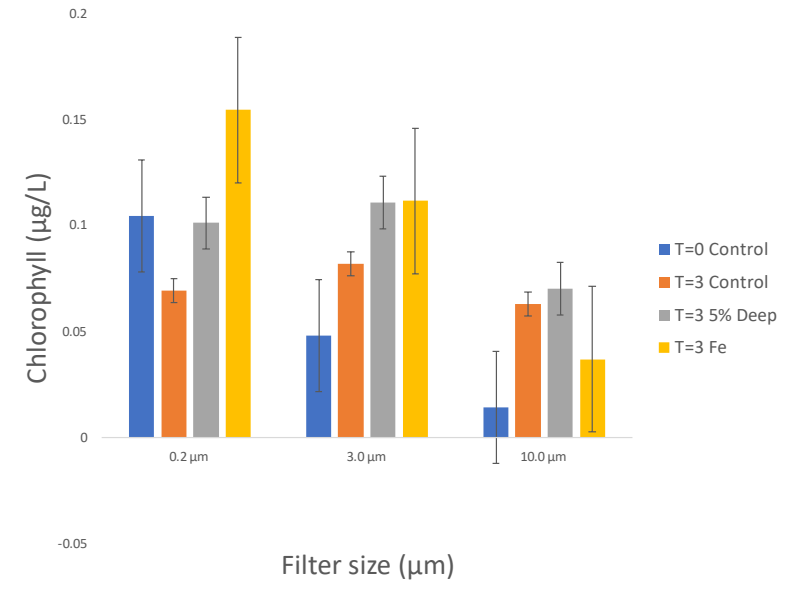

Figure 6.c. Chlorophyll incubation response data from Stations 2, 9, and 16. T1-4 were recorded in 24-hour increments. Size fractionation as represented by filter size on the axis displays data of chlorophyll processed by their representative filters. 5% deep correlates with water taken from below the mixed layer where chlorophyll concentrations are largely homogenous. Treatments from Iron and Nitrate are statistically significant from control meaning their chlorophyll response was greater than the difference of 5% deep and 5% deep and the experimental nutrient variable.

The 5% Deep treatment group had the largest increase in chlorophyll concentration relative to the control group at the 0.2 µm and 3.0 µm filter sizes. In contrast, the Fe treatment group had the largest increase in chlorophyll concentration relative to the control group at the 10.0 µm filter size. The 5% deep treatment was 46.1% and 35.6% higher than the control with the 0.2- and 3.0 µm filters, while the Fe treatment was 47.7 and 36.5 percent higher than the

control with the 0.2 and 3.0 µm filters. The 10 µm filter was only 11.6% more than the control in the 5% deep treatment and 41.2% less than the control for the Fe treatment.

Discussion

This data supports the hypothesis that primary producers in the western equatorial Pacific, an anomalous HNLC area, are limited by one or more nutrients in the water below the mixed layer. When spiking in the incubation bottles within a 19:1 mixture of deep water, chlorophyll concentrations grew more than they did without any additional nutrient spike. This suggests that the primary producers in the surface layer and mixed layer a limited by one or more nutrients and, when given those nutrients, will continue to increase in concentration.

The results suggest that the addition of nutrients, specifically iron and deep water, significantly impacted chlorophyll concentration in the western equatorial Pacific. The "5% Deep" treatment group had the highest percent increase in chlorophyll concentration relative to the "control" group. In comparison, the "Fe" treatment group had a lower percent increase compared to the "5% Deep" treatment group but still had a substantially higher increase than the "control" group. The Fe treatment group showed a different response compared to the other treatment groups, which may indicate a more complex relationship between iron and chlorophyll production. The findings support the original hypothesis that supplementing iron to water taken from the western equatorial Pacific increases the concentration of primary producers. Further research could be done to investigate the underlying mechanisms behind the observed responses and to determine the long-term effects of nutrient additions on primary production in the western equatorial Pacific.

Specifically, the results from Station 2 show that both the "5% Deep" and "Fe" treatment groups had significantly higher chlorophyll concentrations compared to the control group, with the "5% Deep" treatment group showing the highest percent increase in chlorophyll concentration. The 0.2 µm filter size had the largest increase in chlorophyll concentration for both the "5% Deep" and "Fe" treatment groups. In comparison, the 10 µm filter size had the largest increase in chlorophyll concentration for the control group.

Results from Station 9 indicate that the Fe treatment group significantly increased chlorophyll concentration compared to the control group over a 96-hour period. The 10.0 µm filter size had the largest increase in chlorophyll concentration in all three treatment groups, consistent with the results from Station 2.

Results from Station 16 show that the "5% Deep" treatment group had the largest increase in chlorophyll concentration relative to the control group at the 0.2 µm and 3.0 µm filter sizes. In contrast, the Fe treatment group had the largest increase in chlorophyll concentration relative to the control group at the 10.0 µm filter size. The Fe treatment group showed a decrease in chlorophyll concentration from T=0 to T=3, in contrast to the other treatment groups that showed an increase. The Fe treatment had a complex effect on chlorophyll concentration, with both increases and decreased observed depending on the filter size. The control group showed a consistent decrease in chlorophyll concentration, with the largest percent decrease at the 0.2 µm filter size (-33.9%). The 5% Deep treatment group showed an overall increase in chlorophyll concentration at all filter sizes, with the largest percent increase at the 10.0 µm filter size (+255.6%). These trends suggest that the Fe treatment may have provided a favorable environment for phytoplankton growth, but the effects varied depending on the phytoplankton size.

Some zones within the Pacific Ocean, such as the waters studied in this experiment, are HNLC due to limiting nutrients correlated to Liebig's law. Liebig's law of the minimum is a principle in ecology that states that the growth and reproduction of a population are limited by the nutrient or environmental factor that is in the shortest supply. This means that even if all other conditions necessary for growth and reproduction are present if one essential factor is lacking, the population will not be able to thrive (Justus von Liebig, 1840).

Some limitations in my experimental design could have contributed to the standard error in the data. Firstly, the lab was not a trace-free metal environment. It is possible that trace metals were introduced during measurements or spiking procedures. Also, as my hypothesis required chlorophyll to grow, I chose to use water from below the mixed layer, which is known to have nutrients that the chlorophyll in the mixed layer requires. Since I decided to use this deep water, albeit partially in my incubations, it is impossible to know which nutrients, without further analysis, was the limiting nutrient. However, when my iron was introduced to the deep water, there was a difference between incubation with DFe and deep water alone.

Overall, these results highlight the complex relationship between nutrient additions and primary production in the western equatorial Pacific, with different treatments resulting in different responses in chlorophyll concentration. Further research is needed to fully understand the mechanisms driving these responses and the long-term effects of nutrient additions on the marine ecosystem in this region.

Conclusions

In the efforts to study and produce more data on this area in the western equatorial Pacific, I provided data supporting my original hypothesis, which resulted in chlorophyll growth using nutrients such as DFe. I hypothesize that the biology in the area of research was limited by nutrients, such as DFe, which is readily scavenged in the mixed layer. This fact and the chemical necessity for iron in photosynthesis narrowed my efforts towards incubating with biogenically available iron, such as FeCl3. However, without recent historical data in this area, my research is the most current data on these same stations and some of the only data that measured chlorophyll and size-fractionated the samples in situ.

Iron is an essential nutrient for marine organisms because it is a critical component of the photosynthetic pigment chlorophyll used by phytoplankton to convert light energy into organic matter through photosynthesis. Iron availability in the ocean can therefore limit the growth of phytoplankton and ultimately impact the entire marine food web, including fish and other marine animals that rely on phytoplankton as a food source. By studying iron in the ocean, we can better understand its role in regulating primary productivity and the marine food web. This information can help us to predict and manage the impacts of climate change, ocean acidification, and other environmental stressors on marine ecosystems. In future research, it would be interesting to see which species of chlorophyll-containing microorganisms respond the most to iron incubations and provide data for computer modeling, which costs a fraction of typical research cruises and is accessible to the public.

Acknowledgments

I want to express my gratitude to all those who have contributed to the success of this research project. First and foremost, I thank the University of Washington and the School of Oceanography for providing the financial support that made this study possible. I also sincerely thank the captain and crew of the Research Vessel, Thomas V. Thompson, for their invaluable assistance in collecting and processing the seawater samples used in this study. I am also grateful to my colleagues who provided technical support and insightful discussions throughout the project.

I thank doctors Rick Keil, Francois Ribalet, Mark Warner, Ginger Armbrust, Kathy Newell, and Andrea Ogston for their constructive feedback on my experimental design and data analysis, which significantly improved the quality of my research. I would also like to thank the laboratory staff members who analyzed the nutrient for their technical assistance and helpful suggestions. Special thanks to the senior oceanography students on the cruise for their tireless efforts in sample preparation, measurements, and data management during their shifts. Finally, I would like to express my heartfelt appreciation to my family and friends for their unwavering support and encouragement throughout my research journey. Their support and encouragement have motivated and inspired me to pursue my scientific endeavors.

References

Caspers, H. (1970). J. D. H. Strickland and T. R. Parsons: A Practical Handbook of Seawater Analysis. Ottawa: Fisheries Research Board of Canada, Bulletin 167, 1968. 293 pp. $ 7.50. *Internationale Revue Der Gesamten Hydrobiologie Und Hydrographie*, *55*(1), 167–167. https://doi.org/10.1002/iroh.19700550118

Emerson, D. (2016). The Irony of Iron – Biogenic Iron Oxides as an Iron Source to the Ocean. *Frontiers in Microbiology*, *6*. https://doi.org/10.3389/fmicb.2015.01502

EL NIÑO/SOUTHERN OSCILLATION (ENSO) DIAGNOSTIC DISCUSSION. Climate prediction center: Enso diagnostic discussion. (2023, January 12). Retrieved January 22, 2023, from https://www.cpc.ncep.noaa.gov/products/analysis_monitoring/enso_advisory/ensodisc.shtml

Gumsley, A. P., Chamberlain, K. R., Bleeker, W., Söderlund, U., de Kock, M. O., Larsson, E. R., & Bekker, A. (2017). Timing and tempo of the Great Oxidation Event. *Proceedings of the National Academy of Sciences*, *114*(8), 1811–1816. https://doi.org/10.1073/pnas.1608824114

Joye, S. B., Bowles, M. W., & Ziervogel, K. (2022). Marine Biogeochemical Cycles. In L. J. Stal & M. S. Cretoiu (Eds.), *The Marine Microbiome* (pp. 623–671). Cham: Springer International Publishing. https://doi.org/10.1007/978-3-030-90383-1_15

LORENZEN, C. J. (1967). DETERMINATION OF CHLOROPHYLL AND PHEO-PIGMENTS: SPECTROPHOTOMETRIC EQUATIONS1. *Limnology and Oceanography*, *12*(2), 343–346. https://doi.org/10.4319/lo.1967.12.2.0343

Lueder, U., Jørgensen, B., Kappler, A., & Schmidt, C. (2020). Photochemistry of iron in aquatic environments. *Environmental Science: Processes & Impacts*, *22*. https://doi.org/10.1039/C9EM00415G

Mondal, S., Samanta, G., & De la Sen, M. (2022). Dynamics of Oxygen-Plankton Model with Variable Zooplankton Search Rate in Deterministic and Fluctuating Environments. *Mathematics*, *10*(10), 1641. https://doi.org/10.3390/math10101641

Morel, F. M. M., & Price, N. M. (2003). The Biogeochemical Cycles of Trace Metals in the Oceans. *Science*, *300*(5621), 944–947. https://doi.org/10.1126/science.1083545

NASA. (2001, July 10). *John Martin*. NASA. Retrieved February 1, 2023, from https://earthobservatory.nasa.gov/features/Martin/martin_4.php

Pham, A., & Ito, T. (2021). Anthropogenic Iron Deposition Alters the Ecosystem and Carbon Balance of the Indian Ocean Over a Centennial Timescale. *Journal of Geophysical Research: Oceans*, *126*. https://doi.org/10.1029/2020JC016475

Ribalet, F., Marchetti, A., Hubbard, K. A., Brown, K., Durkin, C. A., Morales, R., et al. (2010). Unveiling a phytoplankton hotspot at a narrow boundary between coastal and offshore waters. *Proceedings of the National Academy of Sciences*, *107*(38), 16571–16576. https://doi.org/10.1073/pnas.1005638107

Rijkenberg, M. J. A., Middag, R., Laan, P., Gerringa, L. J. A., van Aken, H. M., Schoemann, V., et al. (2014). The Distribution of Dissolved Iron in the West Atlantic Ocean. *PLoS ONE*, *9*(6), e101323. https://doi.org/10.1371/journal.pone.0101323

Schoffman, H., Lis, H., Shaked, Y., & Keren, N. (2016). Iron–Nutrient Interactions within Phytoplankton. *Frontiers in Plant Science*, *7*. https://doi.org/10.3389/fpls.2016.01223

Underwood, E. (2020, January 3). *The complicated role of iron in Ocean Health and Climate Change*. Smithsonian.com. Retrieved February 1, 2023, from https://www.smithsonianmag.com/science-nature/complicated-role-iron-ocean-health-and-climate-change-180973893/

Von der Heyden, B., Roychoudhury, A., Mtshali, T., Tyliszczak, T., & Myneni, S. (2012). Chemically and Geographically Distinct Solid-Phase Iron Pools in the Southern Ocean. *Science (New York, N.Y.), 338*, 1199–201. https://doi.org/10.1126/science.1227504

Von Liebig, J. (1840). *Die organische Chemie in ihrer Anwendung auf Agricultur und Physiologie*. Vieweg.

Weber, T. (2020). Southern Ocean Upwelling and the Marine Iron Cycle. *Geophysical Research Letters*, *47*(20). https://doi.org/10.1029/2020GL090737